

Active Pt-PbO_x/C Anodes to Promote the Formic Acid Oxidation in Presence of Sulfuric Acid

Guilherme S. Buzzo,^a Rafael V. Niquirilo^a and Hugo B. Suffredini^{*a}

^aCentro de Ciências Naturais e Humanas, Universidade Federal do ABC,
Rua Santa Adélia, 166, Bairro Bangu, Santo André-SP, Brazil

Este trabalho propõe estudar ânodos baseados em Pt e PbO_x frente à reação de oxidação do ácido fórmico. Os materiais estudados foram sintetizados por uma metodologia sol-gel adaptada. Estudos voltamétricos mostraram que o processo de oxidação ocorre em potenciais extremamente baixos. Este bom desempenho foi comprovado por meio de curvas de polarização e cronoamperometrias.

The performance of Pt-PbO_x-based catalysts to promote the formic acid oxidation is described here. All materials were synthesized by a modified sol-gel method. Voltammetric studies showed that the Pt-PbO_x/C anode starts the oxidation process at extremely low potentials. Quasi-stationary polarization experiments and current vs. time measurements confirmed this affirmation.

Keywords: lead oxide-based catalysts, Pb, formic acid oxidation, modified sol-gel method, energy.

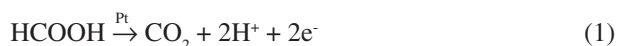
Introduction

Direct formic acid fuel cells are promising devices for the production of electrical energy in portable devices. Formic acid is non-inflammable liquid, used as additive in food and its transportation are less dangerous than for aliphatic alcohols.¹ On the other hand, formic acid is corrosive and its storage must be done with discretion.

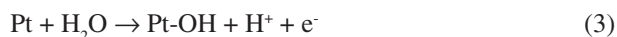
Compared specifically with methanol, other advantage of using formic acid is the lower cross-over effect through the polymer membrane. For this reason, the concentration of the fuel can achieve about 20 mol L⁻¹ of concentration for the formic acid and only 2 mol L⁻¹ for the methanol, due to the problems related with the Nafion® membrane.² Taking this factor into account, the power density of direct formic acid fuel cells (DFAFC) is higher than that observed for DMFC, despite the energy density of methanol being a third higher than that of formic acid.³

Several oxidation mechanisms were proposed concerning the formic acid oxidation. One of the most accepted mechanisms is presented below. The formic acid oxidation can undergo two parallel pathways on platinum (with or without the CO adsorption step).⁴ In the first one,

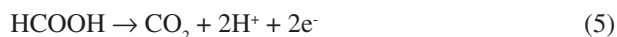
called the “direct pathway”, the acid is directly oxidized to carbon dioxide:



In the second possibility, the mechanism occurs by one chemical and two electrochemical steps, initialized with the CO adsorption on the Pt surface:



The overall reaction is



Several reports appear in the literature concerning formic acid oxidation. Lee *et al.* studied the effect of the Au composition for formic acid oxidation on AuPt catalysts, using a linear sweep voltammetry technique in a 0.5 mol L⁻¹ H₂SO₄ + 1 mol L⁻¹ HCOOH solution.⁵ In another study, Uhm *et al.* demonstrated the utilization of electrochemical impedance spectroscopy to compare the

*e-mail: hugo.suffredini@ufabc.edu.br

performance of DMFC and DFAFC systems.⁶ Selvaraj *et al.* reported the high efficiency of a catalyst based on Pt and PtPd to promote formic acid and formaldehyde oxidation,⁷ while Jeong *et al.* discussed the cross-over affect in direct formic acid fuel cells.⁸

In the 1970's, Adzic and co-authors published important papers related to this subject.⁹⁻¹¹ In one of these studies, the authors observed the increase of the catalytic response, using a Pt-Pb system synthesized by the UPD technique, and compared the results with a bare Pt electrode.¹⁰ Other systems studied by the same authors are related to the catalytic performance of foreign noble metals, Pd monolayers on Pt, and the application of pulsing potentials to avoid the poisoning effects related to formic acid oxidation. Other UPD systems were studied by different authors.¹²⁻¹⁶

More recently, Pd and Pd alloys have appeared in the literature with very interesting results.¹⁷⁻¹⁹ Following this subject, Waszczuk *et al.* synthesized nanoparticles containing Pd, Ru and Pt.²⁰ In this study, the Pt/Pd catalyst shows the best performance. Casado-Rivera *et al.* observed that a significant number of the ordered intermetallic phases exhibited enhanced electrocatalytic activity when compared to that of Pt, in terms of both oxidation onset potential and current density, in particular, PtPb electrodes.²¹ Tripkovic *et al.* demonstrated that a PtBi catalyst starts formic acid oxidation at 0.25 V less positive potential, in comparison with polycrystalline Pt.²²

As demonstrated, the synergetic effects of lead in anodes have been widely discussed in the literature, but the use of lead oxides (PbO_x) to promote formic acid oxidation are being presented and discussed for the first time in this paper.

In order to produce the catalysts, several techniques of deposition have been proposed to fix Pt, other metals or metallic oxides onto different substrates. One of the most widely used techniques was proposed by Bönemann.²³ Some reports published recently demonstrated that an adaptation of the traditional sol-gel constitutes an efficient and simple technique to produce anodes containing Pt, Ru and Pb with the desired composition.^{24,25}

Thus, the aim of this work is to use these previously prepared catalysts, deposited by the sol-gel method on carbon powder and fixed on a glassy carbon substrate, to promote formic acid oxidation in the presence of sulfuric acid. The physical characterization of this material (performed by X-ray diffraction (XRD) and energy dispersive X-ray (EDX) analysis) was described in a previous work.²⁵ The electrochemical studies of formic acid oxidation were carried out by cyclic voltammetry, chronoamperometry and *quasi*-stationary polarization curves, carried out in potentiostatic mode (Tafel plots).

Experimental

Reagent, apparatus and preparation of the precursors

A conventional one compartment Pyrex[®] glass cell provided with three electrodes was used to promote all electrochemical studies. The cell was constituted by the Hydrogen Electrode in the Same Solution (HESS) as reference, a Pt foil (2 cm²) as auxiliary and a glassy carbon as working electrode, as support for the modified powders. The substrate was previously polished with alumina and washed with isopropyl alcohol. The supporting electrolyte was a H₂SO₄ 0.5 mol L⁻¹ solution (Merck[®]) also containing, in some cases, formic acid 1.0 mol L⁻¹ (Synth[®]). The electrochemical measurements were carried out using an AUTOLAB PGSTAT 100 equipment.

The preparation of the precursors is described below. As an example, the platinum solution was prepared adding 9.9 x 10⁻³ g of the Pt (II) acetylacetonate (Aldrich[®]) to 25 mL of a liquid mixture constituted by ethanol (Synth[®] 98[°]) and acetic acid (Merck[®] P.A.) 3:2 (v/v), while the lead and ruthenium solutions were prepared using the same procedure but adding the necessary acetylacetonates quantities (Aldrich[®]). The final concentration of each solution was 1.0 x 10⁻³ mol L⁻¹. The carbon black powder used was Vulcan[®] XC72R, and 5% commercial Nafion[®] solution (DuPont) was purchased from Aldrich[®]. The normalization of the currents were carried out according to the mass of Pt deposited on the carbon powder for the Pt-PbO_x/C and Pt-(PbO_x-RuO₂)/C catalysts (generating pseudo-current densities) or considering the quantity of 2.0 x 10⁻⁹ mol Pt cm⁻¹ (medium value for polycrystalline Pt) for the working polycrystalline Pt electrode (geometric area = 2.0 cm², roughness factor = 4.5, real area = 9 cm²). The roughness factor was determined by the hydrogen desorption process on the Pt electrode in sulfuric acid.

Modified Carbon Powder Preparation

The composites containing Pt, Ru, Pb and C were prepared using fixed mass proportion of metals Pt:Pb (50:50), Pt:Ru:Pb (50:25:25) and carbon powder as a support. The catalyst mass load was fixed at 10% with respect to the carbon powder.

All depositions were carried out according to a procedure reported elsewhere,²⁵ by putting the dry carbon powder (0.13 g) into a beaker and covering this powder with small amounts of the solutions (1 to 2 mL by step), producing a "black mud" without excess liquid. After the quasi-total evaporation of the liquid from the "black mud" (at room temperature) further amounts of liquid were

added in 1 mL aliquots. This procedure was repeated until a load of 10% catalysts was attained. The carbon powder was then subjected to a thermal treatment at 400 °C for 1 h under an argon atmosphere, to avoid the oxidation of the C to CO₂.

It is important to observe that the suspension of the particles (or the formation of a colloidal solution) was not controlled. So, the kind of solution studied in this work cannot be called as “sol”. It is not possible to conclude that the modification of the carbon black represents a direct sol-gel modification. Thus, the process is an adaptation of the traditional sol-gel process.

Fixation of the powder onto a glassy carbon substrate

The synthesized composites were fixed onto a glassy carbon electrode (geometric area = 0.5 cm²), following the procedure described firstly by Schmidt *et al.*²⁶ Firstly, a 5 wt.% Nafion solution was diluted ten times in deionised water. Then, 0.008 g of the composite was added to 1 mL of water and 0.20 mL of the diluted Nafion[®] solution. The resulting system was placed in an ultrasonic bath for 3 min to disperse the powder in the Nafion[®] solution. Finally, 0.02 mL of the obtained dispersion was transferred onto a glassy carbon electrode with geometric area of 0.125 cm². The deposited suspension was then dried for 60 min at 80 °C to complete evaporation of the solvents.

Results and Discussion

Physical Characterization

As previously noted, the Pt-PbO_x/C and Pt-(PbO_x-RuO₂)/C catalysts were the same used to promote the ethanol oxidation in a recent publication.²⁵ The materials were previously characterized by X-ray diffraction (XRD) to verify the presence of the oxides and metal onto a carbon powder, determining *a posteriori* the crystallite dimensions using WinFit 1.0 software and energy dispersive X-ray analysis (EDX) to promote a semi-quantitative determination of the metals in the catalysts.

In short, the XRD patterns obtained for all composites prepared in this work, together with the corresponding indication of the main peaks and their identification by comparison with the JCPDS (Joint Committee of Power Diffraction Standards) cards, are presented. The Pt was deposited as a metal in the polycrystalline form, showing the peaks corresponding to the main three crystallographic planes (111), (200) and (220). Ruthenium was deposited as RuO₂ and, in addition, Pb was deposited as a mixture of PbO and PbO₂. Thus, the nomenclature of all Pb containing

compounds is designated by “PbO_x”. The EDX analyses revealed that Pb is preferentially deposited in relation to Pt, while for the other composites that were studied, a very good agreement between the experimental and the expected theoretical values is observed. Furthermore, the values of the crystallite dimensions obtained with the software ranged from 3.5 nm to 4.0 nm for all compounds.

Electrochemical Studies

Figure 1 shows the cyclic voltammetric responses studies carried out in H₂SO₄ 0.5 mol L⁻¹ + HCOOH 1.0 mol L⁻¹ solution for polycrystalline Pt (a), Pt/C (b), Pt-PbO_x/C (c) and Pt-(PbO_x-RuO₂)/C (d). The inserts of the figures represents the electrochemical responses in H₂SO₄ 0.5 mol L⁻¹. The presence of Pt in both lead-based catalysts can be observed due to the inhibited signals of the adsorption-desorption of hydrogen on the exposed Pt in each material. It is important to observe this process, as it is a fundamental parameter that confirms there are no problems (such as potential dislocation) with the reference electrode.

In this way, Figure 1(a) presents the electrochemical responses (after 3 cycles) for the polycrystalline Pt. This material starts the formic acid oxidation at about 0.4 V *vs.* HESS, presenting inhibited oxidation currents, due to the strong CO adsorption process (Eq. 2). In fact, several authors mentioned that formic acid oxidation occurs by the indirect route on polycrystalline Pt, with chemical adsorption of CO on the electrode surface.²⁻⁴ The CO oxidation can be observed at about 0.9 V *vs.* HESS, making polycrystalline Pt unviable as an anode in DFAFC's. In the same way, Figure 1 (b) shows the response of a Pt/C catalyst (10% of catalyst load), synthesized by a modified sol-gel method. The electrochemical behavior is quite similar to that observed with the polycrystalline Pt electrode (Figure 1a) starting the reactions at the same potentials, indicating that the oxidation also occurs by the CO adsorption mechanism. The Pt/C anode was studied because it represents a more realistic system to be used in a real fuel cell system.

A good novelty can be found in Figure 1(c), which shows that the Pt-PbO_x/C anode starts the formic acid oxidation at very low potentials (showing important oxidation currents at the start of the process). The Pt-PbO_x/C catalyst starts the oxidation process at about 0.2 V *vs.* HESS, about 200 mV less positive when compared with polycrystalline Pt, presenting very high formic acid oxidation currents. The CO desorption oxidation peak is not important in this case (at about 0.9 V *vs.* HESS), indicating that the reaction probably occurs by the direct pathway (Eq. 1). As mentioned, Tripkovic *et al.* observed that the

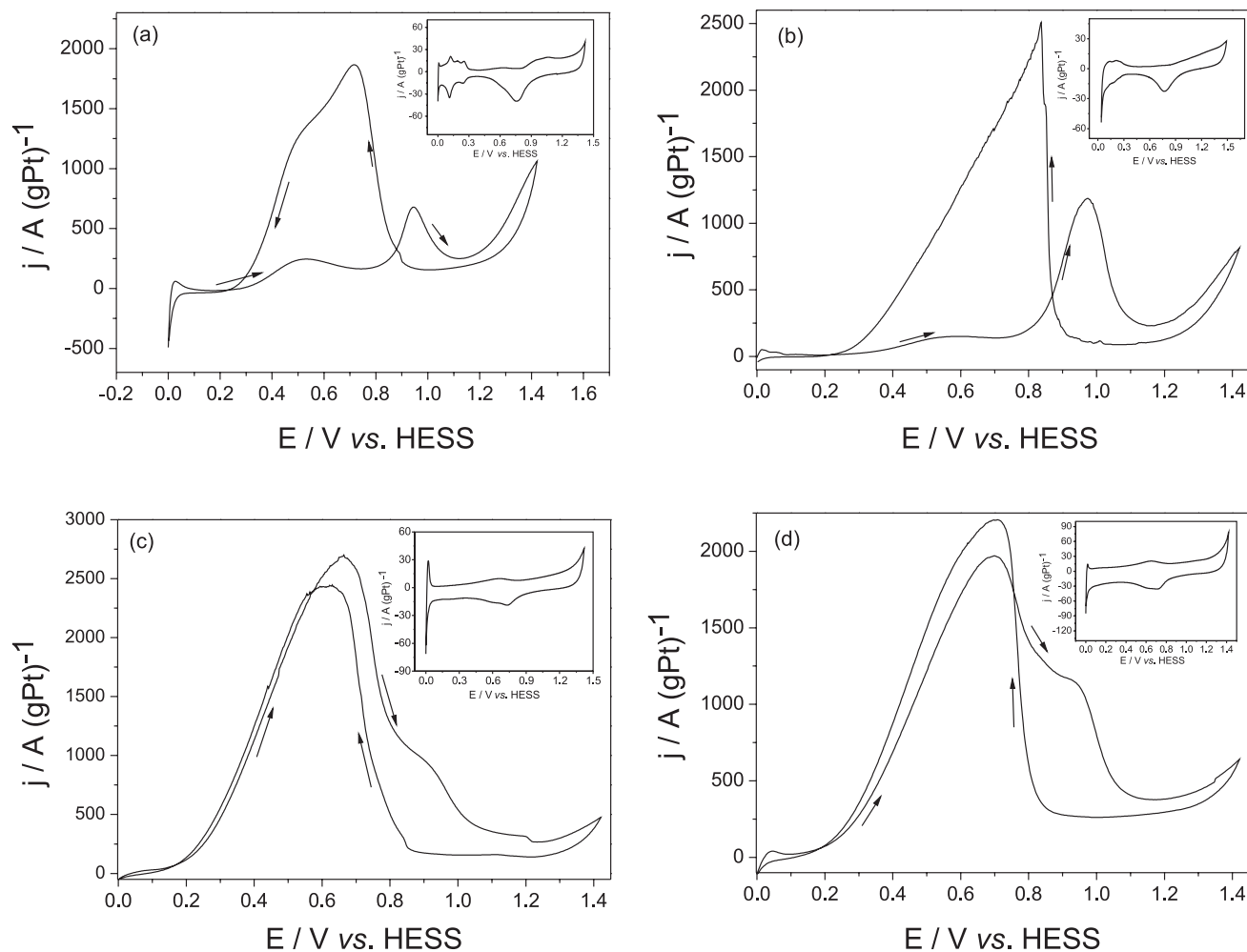


Figure 1 – Cyclic voltammograms (after three cycles) carried out in H_2SO_4 0.5 mol L^{-1} + HCOOH 1.0 mol L^{-1} solution for polycrystalline Pt (a), Pt/C (b), Pt-PbO_x/C (c) and Pt-(PbO_x-RuO₂)/C (d). $v = 20$ mVs⁻¹. All inserts represent the electrochemical responses in H_2SO_4 0.5 mol L^{-1} .

catalysts based in PtBi and PtPb present very good catalytic activity for formic acid oxidation, but these materials have no practical applications in DFAFCs, due to the applied methodology of synthesis (underpotential deposition of Pb in Pt).²² Thus, the use of PbO_x/C as catalyst can be a good choice in real fuel cell systems. The voltammetry profile of the Pt-PbO_x/C catalyst can be compared with metallic Pd, which constitutes the state-of-the-art material to this kind of application.¹⁷⁻¹⁹

Concerning the Pt-(PbO_x-RuO₂)/C catalyst, it is possible to observe in Figure 1(d) that the curve did not present significant differences when compared with the Pt-PbO_x/C anode. The Pt-(PbO_x-RuO₂)/C catalyst presents only about 82% of the pseudo-currents densities when compared with the Pt-PbO_x/C anode in the same conditions. The increase of the oxidation process at about 0.9 V vs. HESS observed for the Pt-(PbO_x-RuO₂)/C can be related to the Ru(II)/Ru(III) transition (dotted line) and similar responses were observed by other authors in different works.²⁷⁻²⁸ Other

possibility is related to the increase of the oxidation of adsorbed carbon monoxide (CO) on the electrode surface when compared with the Pt-PbO_x/C anode. Abruña and co-authors have studied the CO oxidation using ordered intermetallic electrodes and the CO oxidation process was observed in that same range of potentials.²⁹ Thus, it is possible to conclude that the RuO₂ can be eliminated from the composition, because is not possible to justify its utilization.

The interesting performance of the anode constituted by Pt-PbO_x/C for the formic acid oxidation encouraged the study in quasi-stationary conditions. To properly determine and compare the onset potential values for the formic acid oxidation, a minimum value of current was fixed. All onset potential values discussed and obtained from Figure 2 were taken at 5.5×10^{-4} A.

Thus, Figure 2 shows the quasi-steady state polarization curves presented as Tafel plots that were carried out in potentiostatic mode, at 20° C in H_2SO_4 0.5 mol L^{-1} +

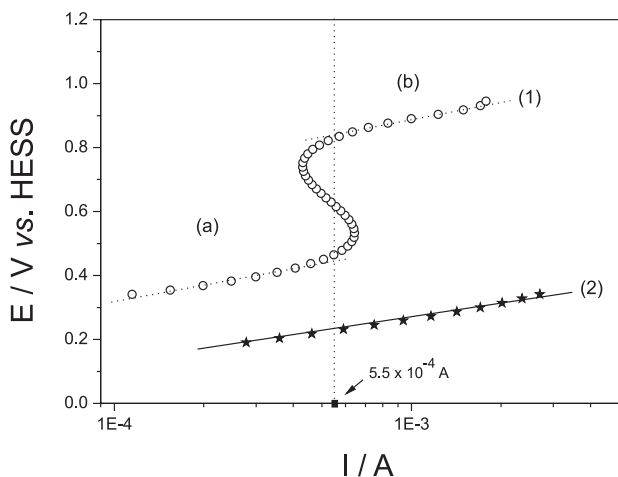


Figure 2 – Tafel Plots recorded in potentiostatic mode in H_2SO_4 0.5 mol L^{-1} + HCOOH 1.0 mol L^{-1} for: Polycrystalline Pt (circles, curve 1) and $\text{Pt-PbO}_x/\text{C}$ (stars, curve 2). $T = 20^\circ\text{C}$. Curve 1 shows two different kinetic-controlled processes: formic acid oxidation (a) and, probably, carbon monoxide oxidation (b).

HCOOH 1.0 mol L^{-1} aqueous solution. It can be observed that the polycrystalline Pt (curve 1) presents two linear Tafel regions. The first one (process “a”), related to the formic acid oxidation, presented a Tafel slope at about 145 mV dec^{-1} , and the onset oxidation potential was 0.44 V vs. HESS at $5.5 \times 10^{-4}\text{ A}$ of current. The second one, probably related to the CO oxidation, showed a Tafel slope of about 150 mV dec^{-1} and an onset oxidation potential of about 0.84 V vs. HESS . In both cases, the rate determining step (rds) is related to a one-electron electrochemical step (Tafel slopes about 120 mV dec^{-1}). In the same way, curve 2 presents the Tafel plot for the $\text{Pt-PbO}_x/\text{C}$ catalyst. In this case the slope was of the order of 128 mV dec^{-1} and the onset potential was about 0.23 V vs. HESS . In agreement with the cyclic voltammetry measurements presented in Figure 1, the $\text{Pt-PbO}_x/\text{C}$ catalyst presented somewhat about 200 mV less positive potential for the formic acid oxidation, in quasi-stationary conditions.

Figure 3 presents current vs. time studies (at 0.3 V vs. HESS) carried out in H_2SO_4 0.5 mol L^{-1} + HCOOH 1.0 mol L^{-1} solution for the $\text{Pt-PbO}_x/\text{C}$ (a), $\text{Pt-(PbO}_x\text{-RuO}_2)/\text{C}$ (b), Pt/C (c) and polycrystalline Pt (d). A low potential was chosen because the system produces many bubbles during the oxidation process for the active materials. The $\text{Pt-PbO}_x/\text{C}$ (a) and $\text{Pt-(PbO}_x\text{-RuO}_2)/\text{C}$ (b) exhibit higher *pseudo-current* densities for the same applied potential at the studied time. On the contrary, the curves related to the Pt/C and polycrystalline Pt tend to zero. Slower and continuous current decays are also observed in the $\text{Pt-(RuO}_2\text{-PbO}_x)/\text{C}$ and $\text{Pt-PbO}_x/\text{C}$ catalysts, due probably to a smaller poisoning of the material as the process advances.

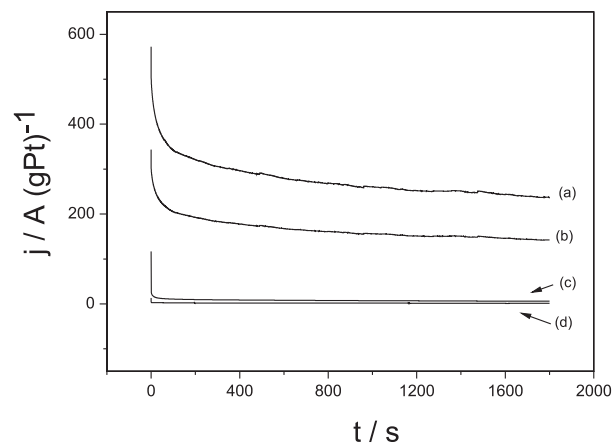


Figure 3 – Current-time responses (at 0.3 V vs. HESS) carried out in H_2SO_4 0.5 mol L^{-1} + HCOOH 1.0 mol L^{-1} solution for $\text{Pt-PbO}_x/\text{C}$ (a), $\text{Pt-(PbO}_x\text{-RuO}_2)/\text{C}$ (b), Pt/C (c) and polycrystalline Pt (d).

Thus, in view of the interesting catalytic activities observed on the $\text{Pt-PbO}_x/\text{C}$ catalyst, further studies will be carried out to understand the oxidation mechanism.

Conclusions

Cyclic voltammetry studies show that the electrochemical oxidation of formic acid presented high *pseudo-current* densities on the $\text{Pt-PbO}_x/\text{C}$ and $\text{Pt-(PbO}_x\text{-RuO}_2)/\text{C}$ catalysts, starting the process at a very low potential, while Pt/C , as expected, cannot be used as an anode in DFAFCs due to the strong CO affinity of the material. The comparison between $\text{Pt-PbO}_x/\text{C}$ and $\text{Pt-(PbO}_x\text{-RuO}_2)/\text{C}$ catalysts demonstrates that RuO_2 does not present any important synergistic effect that justifies its utilization.

Moreover, quasi-steady state polarization curves confirmed that the $\text{Pt-PbO}_x/\text{C}$ catalyst started the oxidation process at very low potentials (0.25 V vs. HESS , somewhat about 200 mV less positive potential for the formic acid oxidation when compared with Pt), presenting a satisfactorily performance to promote formic acid oxidation in *quasi-stationary* conditions. On the contrary, the polycrystalline Pt and Pt/C anodes show a non-synergic behavior, due to the strong affinity of CO to this metal. Finally, the current-time measurements indicate that the $\text{Pt-PbO}_x/\text{C}$ catalyst could be an interesting material to be used as anode in direct formic acid fuel cell systems, presenting a stationary *pseudo-current* density of about 250 A (gPt)^{-1} after 1500 s of oxidation at 0.3 V vs. HESS .

Acknowledgments

We thank FAPESP (2007/05155-1), CNPq (472476/2008-4 and 301863/2008-3), CAPES and UFABC-PRPG for providing G.S. Buzzo and R.V. Niquirilo with scholarships.

References

1. Wang, X.; Tang, Y.; Gao, W.; Lu, T.; *J. Power Sources* **2008**, *175*, 784.
2. Rhee, Y. W.; Ha, S. Y.; Masel, R. I.; *J. Power Sources* **2003**, *117*, 35.
3. Zhu, Y. M.; Ha, S. Y.; Masel, R. I.; *J. Power Sources* **2004**, *130*, 8.
4. Rice, C.; Ha, S.; Masel, R. I.; Wieckowski, A.; *J. Power Sources* **2003**, *115*, 229.
5. Lee, J. K.; Lee, J.; Han, J.; Lim, T-H.; Sung, Y-E.; Tak, Y. *Electrochim. Acta* **2008**, *53*, 3474.
6. Uhm, S.; Chung, S. T.; Lee, J. *J. Power Sources* **2008**, *178*, 34.
7. Selvaraj, V.; Alagar, M.; Kumar, K. S.; *App. Catal. B* **2007**, *75*, 129.
8. Jeong, K-J.; Miesse, C. M.; Choi, J-H.; Lee, J.; Han, J.; Yoon, S. P.; Nam, S. W.; Lim, T-H.; Lee, T. G. *J. Power Sources* **2007**, *168*, 119.
9. Adzic, R. R.; Simic, D. N.; Drazic, D. M.; Despic, A. R.; *J. Electroanal. Chem. Interf. Electrochem.* **1975**, *61*, 117.
10. Adzic, R. R., Simic, D. N., Despic, A. R., Drazic, D. M. *J. Electroanal. Chem.* **1977**, *80*, 81.
11. Adzic, R. R.; O'Grady, W. E.; Srinivasan, S.; *J. Electrochem. Soc.* **1981**, *128*, 1913.
12. Beltowska-Brzezinska, M.; Heitbaum, J.; Vielstich, W.; *Electrochim. Acta* **1985**, *30*, 1465.
13. Campbell, S. A.; Parsons, R. *J. Chem. Soc. Faraday Transactions* **1992**, *88*, 833.
14. Kelaidopoulou, A.; Abelidou, E.; Kokkinidis, G.; *J. Appl. Electrochem.* **1999**, *29*, 1255.
15. Lei, H. W.; Hattori, H.; Kita, H.; *Electrochim. Acta* **1996**, *41*, 1619.
16. Mikhailova, A. A.; Osetrova, N. V.; Vasilev, Y. B.; *Soviet Electrochem.* **1989**, *25*, 1612.
17. Ha, S.; Larsen, R.; Masel, R. I.; *J. Power Sources* **2005**, *144*, 28.
18. Larsen, R.; Zakzeski, J.; Masel, R. I.; *J. Electrochem. Solid-State Lett.* **2005**, *8*, 291.
19. Zhu, Y. M.; Khan, Z.; Masel, R. I.; *J. Power Sources* **2005**, *139*, 15.
20. Waszczuk, P.; Barnard, T. M.; Rice, C.; Masel, R. I.; Wieckowski, A.; *Electrochem. Commun.* **2002**, *4*, 599.
21. Casado-Rivera, E.; Volpe, D. J.; Alden, L.; Lind, C.; Downie, C.; Vazquez-Alvarez, T.; Angelo, A. C. D.; DiSalvo, F. J.; Abruña, H. D.; *J. Am. Chem. Soc.* **2004**, *126*, 4043.
22. Tripkovic, A. V.; Popovic, K. Dj.; Stevanovic, R. M.; Socha, R.; Kowal, A. *Electrochem. Commun.* **2006**, *8*, 1492.
23. Bonnemann, H.; Brijoux, W.; Brinkmann, R.; Dinjus, E.; Fretzen, R.; Jouben, T.; Korall, B.; *J. Molec. Cat.* **1992**, *74*, 323.
24. Suffredini, H. B.; Salazar-Banda, G. R.; Avaca, L. A.; *J. Sol-Gel Sci. Technol.* **2009**, *49*, 131.
25. Suffredini, H. B.; Salazar-Banda, G. R.; Avaca, L. A.; *J. Power Sources* **2007**, *171*, 355.
26. Schmidt, T. J.; Gasteiger, H. A.; Stab, G. D.; Urban, P. M.; Kolb, D. M.; Behm, R. J.; *J. Electrochem. Soc.* **1998**, *145*, 2354.
27. Terezo, A. J.; Pereira, E. C.; *Mater. Lett.* **2002**, *53*, 339.
28. Mattos-Costa, F. I.; de Lima-Neto, P.; Machado, S. A. S.; Avaca, L.A. *Electrochim. Acta* **1998**, *44*, 1515.
29. de-los-Santos-Álvarez, N.; Alden, L. R.; Rus, E.; Wang, H.; DiSalvo, F. J.; Abruña, H. D.; *J. Electroanal. Chem.* **2009**, *626*, 14.

Received: July 3, 2009

Web Release Date: October 23, 2009

FAPESP helped in meeting the publication costs of this article.